INTERNATIONAL SYMPOSIUM ON
DAMs IN A GLOBAL ENVIRONMENTAL CHALLENGES
Bali, Indonesia, June 1ST – 6TH, 2014

Effects of limited number of slip circles and arbitrary slip circles on sliding deformation of embankment dams due to earthquakes

Sho FUJIKAWA, Hiroyuki SATO & Yasufumi ENOMURA
Public Works Research Institute, Tsukuba, Japan
s-fujikawa44@pwri.go.jp

ABSTRACT:
Evaluation of seismic performance of dams is important. According to "Guidelines for Seismic Performance Evaluation of Dams against Large Earthquakes (Draft)" issued by the River Bureau of the Ministry of Land, Infrastructure, Transport and Tourism in Japan in March 2005, sliding deformation is identified one of the most important issues in the evaluation of seismic performance of embankment dams.
To calculate sliding deformation, static analysis of embanking and impounding processes is firstly performed to evaluate static stress distribution. Seismic response analysis is secondly performed and finally sliding deformation analysis is conducted.
To evaluate sliding deformation of embankment dams due to earthquakes, Newmark's method is widely used. In the sliding deformation analysis, number of slip circles is generally restricted due to capacity of computer and a few dozens of slip circles has been used in many previous researches. However, similar to the static sliding stability analysis, method for arbitrarily searching a circle of maximum sliding deformation is also desirable in Newmark's method. Therefore, we conducted a research to investigate the effects of the limited number of slip circles and the arbitrary slip circles on sliding deformation of embankment dams based on Newmark's method due to earthquakes for a model dam of an earth core rockfill dam.
We compared the results between the limited number of slip circles and the arbitrary slip circles, and we confirmed that the maximum sliding deformation of the arbitrary slip circles was larger than that of the limited number of slip circles.

Keywords: Rockfill dam, Newmark's method, sliding deformation, arbitrary slip circles

1. INTRODUCTIONS

The evaluation of seismic performance of dams plays an important role in dam risk management. "Guidelines for Seismic Performance Evaluation of Dams against Large Earthquakes (Draft)" issued by the River Bureau of the Ministry of Land, Infrastructure, Transport and Tourism in Japan in March 2005, (hereinafter, "The Guidelines (Draft)") stipulates that the seismic performance of a dam must maintain its reservoir functions, because when an uncontrollable release of reservoir water is caused by large earthquake motion, the region along the downstream river is in danger of disastrous damage. According to the Guidelines (Draft), the seismic performance of an embankment dam is evaluated by sliding deformation as a basic evaluation index to confirm that there is no danger of reservoir water overflowing the dam and that there is no danger of seepage

failure of embankment dams. Therefore, the sliding deformation during a large earthquake is an important index for the evaluation of seismic performance of embankment dams.

A method widely used to calculate the sliding deformation of an embankment dam during an earthquake is to firstly perform static analysis considering the embanking and impounding processes to calculate the static stress before the earthquake, then performing seismic response analysis and using the results of the seismic response analysis to calculate the sliding deformation by the Newmark's method. (Yamaguchi et al., 2009)

Regarding the method used to set the slip circles to calculate the sliding deformation based on the Newmark's method, because the number of slip circles is generally restricted due to capacity of computer, a few dozens of slip circles has been used in many previous researches. (Yamaguchi et al., 2005) However, similar to the static sliding stability analysis, the method for arbitrarily searching a circle of the maximum sliding deformation is also desirable in the Newmark's method.

Therefore, in this paper, we conducted a research to investigate the effects of the limited number of slip circles and the arbitrary slip circles on the sliding deformation of embankment dams based on the Newmark's method due to earthquakes for a model dam of an earth core rockfill dam.

2. SLIDING DEFORMATION ANALYSIS DURING AN EARTHQUAKE BASED ON THE NEWMARK'S METHOD

2.1 Outline of the analysis method

Embanking analysis and impounding analysis were done to obtain the static stress before the earthquake, then seismic response analysis was performed based on the equivalent linearization method.

In order to account for the non-linear properties of embankment dam body materials in the embanking analysis, non-linear elastic analysis based on the Duncan-Chang model was performed. (Duncan et al., 1970) Next, the impounding analysis was conducted to obtain the seepage force and buoyancy in the embankment dam body during impounding. The embanking analysis results and impounding analysis results were superimposed to calculate the static stress and deformation before the earthquake. The initial shear modulus calculated based on the initial stress of the embankment dam body and the dynamic deformation properties were used to perform the seismic response analysis, calculating the response acceleration of the embankment dam body caused by the earthquake.
Later, the time history of average values of the response acceleration of the sliding soil mass inside a circle was used to calculate the sliding deformation during the earthquake based on the concept of the Newmark's method. (Newmark, 1965) Hereinafter, this series of analysis methods will be called the Newmark's method.

2.2 Analysis Model

The analysis model of an earth core rockfill dam with a height of 100m and the crest width of 10m shown in Figure 1 is used. The upstream and downstream slope gradients of the core and filter zones were 1:0.2 and 1:0.35, respectively. The upstream and downstream slope gradients of the rock zones were decided according to the static sliding stability

analysis based on the seismic coefficient method. The seismic coefficient k of 0.15 and reservoir water level which was 92% of the dam height are used and the minimum safety factor is 1.2 in the seismic coefficient method. As a result of the static sliding stability analysis, the slope gradients on the upstream and the downstream sides of the rock zones were 1:2.7 and 1:1.9, respectively. Table 1 shows the physical properties of the dam body materials used for the static sliding stability analysis. The shear strength was evaluated based on the c-φ method and the cohesion, c, of the materials was set as zero using the design values of an existing earth core rockfill dam.

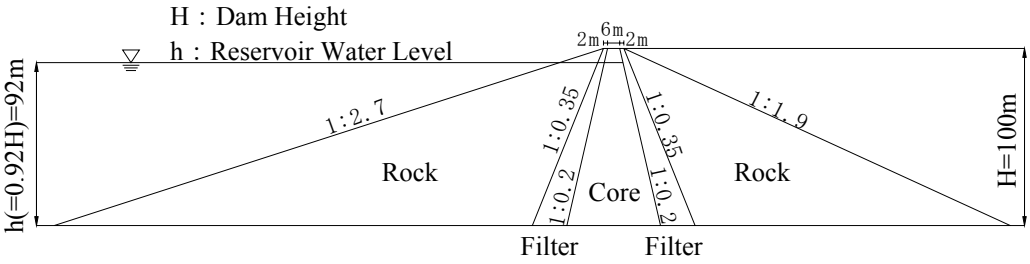

Figure 1. Analysis model (dam body part)

Table 1. Input physical properties for static sliding stability analysis

Material	Wet Density ρ_t (t/m^3)	Saturated Density ρ_{sat} (t/m^3)	Cohesion c (kN/m^2)	Internal Friction Angle φ (°)
Core	2.07	2.10	0	36.0
Filter	2.08	2.15	0	37.0
Rock	2.01	2.11	0	41.5

Figure 2 shows the elements of the embanking analysis model. The modeling range of the foundation was approximately 3 times the dam base length in the horizontal direction and approximately 2 times the dam height in the vertical direction. For the embanking analysis, the dam body and foundation were modeled. For the seepage flow analysis, the core zone and upstream rock and filter zones was modeled. For the seismic response analysis and the sliding deformation analysis, the dam body was modeled.

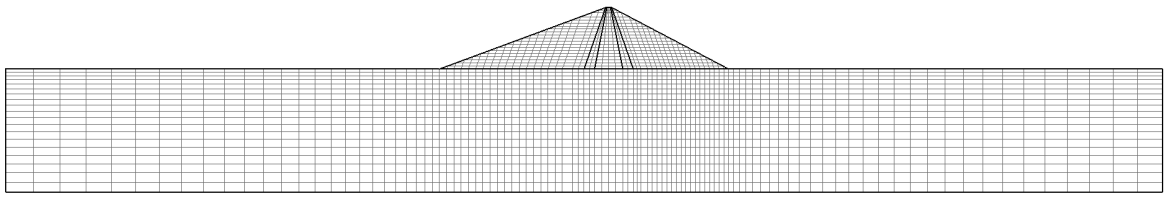

Figure 2. Elements for embanking analysis

2.3 Embanking analysis

Table 2 shows the parameters of the Duncan-Chang model and the material properties used for the embanking analysis. The material properties were the design values of an existing earth core rockfill dam in Japan. The foundation was presumed to have linear deformation properties. Boundary conditions of the foundation were vertical roller for the side boundaries and fixed for the bottom.

Table 2. Material properties for the embanking analysis

Material	Physical properties		Static deformation properties						Shear strength properties	
	Wet Density ρ_t (t/m^3)	Saturated Density ρ_{sat} (t/m^3)	Elastic Modulus E_t			Poisson's Ratio v_t			Cohesion c (kN/m^2)	Internal Friction Angle φ (°)
			K	n	Rf	G	F	D		
Core	2.07	2.10	281.6	0.564	0.785	0.342	0.1	8.3	15.2	36.0
Filter	2.08	2.15	947.2	0.317	1.042	0.303	0.344	7.21	23.5	37.0
Rock	2.01	2.11	1073.5	0.131	0.744	0.24	0.183	10.68	64.7	41.5
Foundation	—		4,312 MN/m^2			0.25			—	

2.4 Impounding analysis

Table 3 and Figure 3 show the properties of the core material used for seepage analysis. The water level was assumed to be 92% of the dam height. The seepage force and buoyancy obtained by the seepage analysis were caused to act on the core, upstream sides both filter and rock zones. For upstream rock and filter zones, which are higher than the seepage surface, the stress was assumed to be unchanged from the embanking analysis.

Table 3. Material properties for seepage analysis

Material	Water Level (m)	Permeability Coefficient k (m/s)	Porosity n
Core	92	1.E-07	0.338

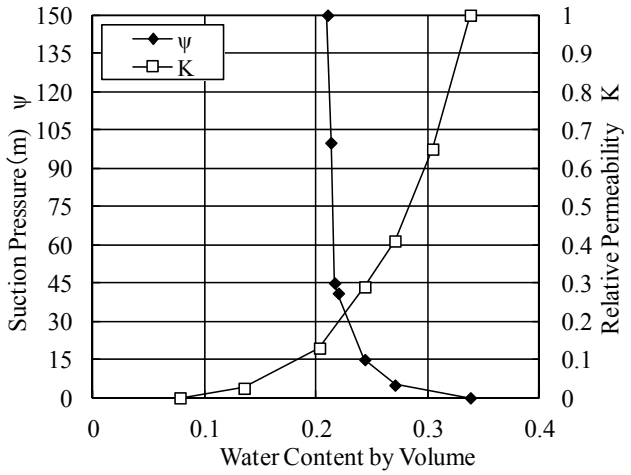

Figure 3. The unsaturated seepage properties of the core material

2.5 Seismic response analysis

Table 4 and Figure 4 show the dynamic deformation properties and the strain dependency properties of the materials used for the seismic response analysis. The dynamic deformation properties were decided based on the dynamic deformation test results obtained from laboratory tests using dam body materials of an existing earth core rockfill dam in Japan. In this paper, elements above the seepage line were considered to be the unsaturated parts, and elements below the seepage line were considered to be the saturated parts. For the saturated part, the material properties of the dynamic deformation properties of the saturated conditions in Table 4 and Figure 4 were used. For the unsaturated part, the properties of unsaturated conditions were used in Table 4 and Figure 4. For the dynamic Poisson's ratios, Sawada's formula was used. (Sawada et al., 1977) In this paper, because

the dam body was only considered for the seismic response analysis, the energy dissipation in the foundation was considered as the equivalent dissipation damping ratio by increasing the material damping ratio uniformly by 15% and the boundary condition of the bottom was fixed.

Table 4. The dynamic deformation properties used for the seismic response analysis

Material		Dynamic deformation properties			
		Initial Shear Modulus G_0 *1	Strain dependency properties *2		Poisson's Ratio ν
		(MN/m^2)	$\gamma \sim G/G_0$	$\gamma \sim h$	
Core	saturated	$335\sigma'_m{}^{0.496}$	γ_r=6.52×10^{-4}	h_{max}=15.6%	
	unsaturated	$295\sigma'_m{}^{0.444}$	γ_r=1.06×10^{-3}	h_{max}=18.0%	
Filter	saturated	$523\sigma'_m{}^{0.580}$	γ_r=4.20×10^{-4}	h_{max}=16.4%	
	unsaturated	$628\sigma'_m{}^{0.665}$	γ_r=4.74×10^{-4}	h_{max}=15.6%	Sawada's formula *3
Rock	saturated	$474\sigma'_m{}^{0.479}$	γ_r=4.45×10^{-4}	h_{max}=13.9%	
	unsaturated	$737\sigma'_m{}^{0.680}$	γ_r=4.80×10^{-4}	h_{max}=14.0%	

*1) σ'_m : Average effective stress after seepage analysis $\sigma'_m = (\sigma_1 + \sigma_3)(1+\nu)/3$

*2) $G/G_0 = 1(1+\gamma/\gamma_r), h = h_{max}(1 - G/G_0)$

*3) $\nu = 0.450 - 0.006Z^{0.60}$: core material

$\nu = 0.375 - 0.006Z^{0.58}$: filter and rock materials (shallower than the seepage line)

$\nu = 0.490 - 0.001Z^{0.95}$: filter and rock materials (depper than seepage line)

Z : depth from the surface of the dam body (m)

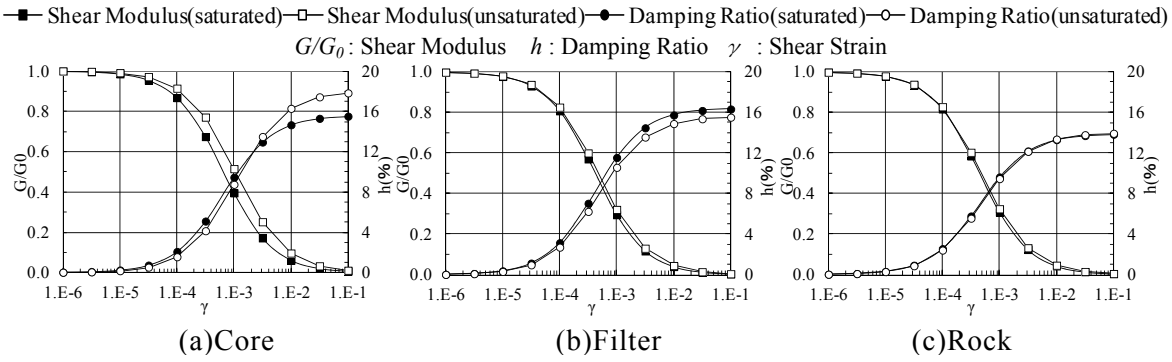

(a)Core (b)Filter (c)Rock

Figure 4. The strain dependency properties of shear modulus and damping ratios

As the input seismic motion, the seismic record observed in the inspection gallery of the Minoogawa dam of an earth core rockfill dam during the Southern Hyogo prefecture earthquake in 1995 was used. Figure 5 shows the seismic motion observed at the Minoogawa dam. In this paper, the maximum acceleration of the time history in the upstream-downstream direction of the seismic motion at the Minoogawa dam was amplified to 1,000gal. The vertical seismic motion at the Minoogawa dam was also amplified using the same multiplier for the upstream-downstream direction seismic motion. The input seismic motion was input from the bottom of the dam body.

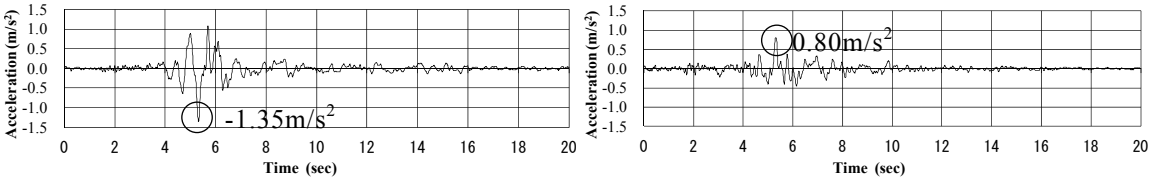

(a)Upstream-Downstream Direction (b)Vertical Direction

Figure 5. Acceleration time histories of the seismic motion observed at the Minoogawa dam

2.6 Method of setting the hypothetical slip circle

The circle used for the sliding deformation analysis during the earthquake was set using the methods of setting the limited number of slip circles and the arbitrary slip circles.

2.6.1 Method of setting the limited number of slip circles

Figures 6 and 7 show a limited number of slip circles that were set in the sliding deformation analysis. A total of 4 circle groups was set, with the circles on the upstream side set as 2 circle groups—shallow circles [1] to [5] and deep circles [6] to [10] as circles which passed only through the rock zone, and at the same time, 2 circle groups—deep circles [11] to [15] and deep circles [16] to [20] as circles which passed through the core zone. The values of y/H were used for the decision of the depths of the circles, where *y* represents circle depth and *H* represents dam height. The values of *y/H* were set at 0.2, 0.4, 0.6, 0.8, and 1.0. A total of 20 circles were used in the upstream side shown in Figure 6. Circles were set similarly for the downstream side so a total of 20 circles were set for the downstream side. The circle groups are called the limited number of slip circles in this paper.

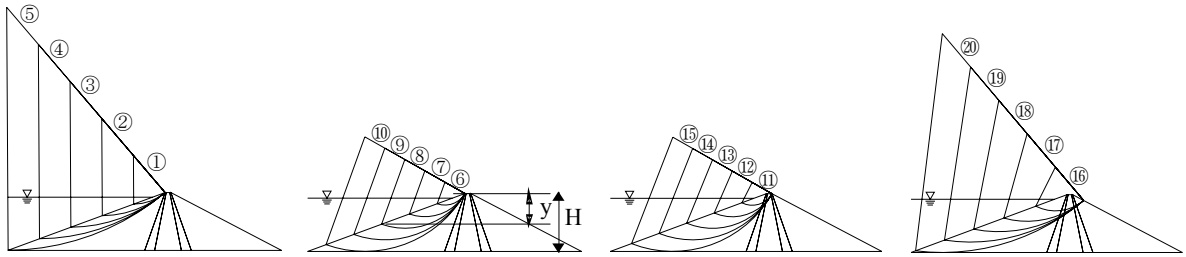

Figure 6. Upstream side slip circles of the limited number of slip circles

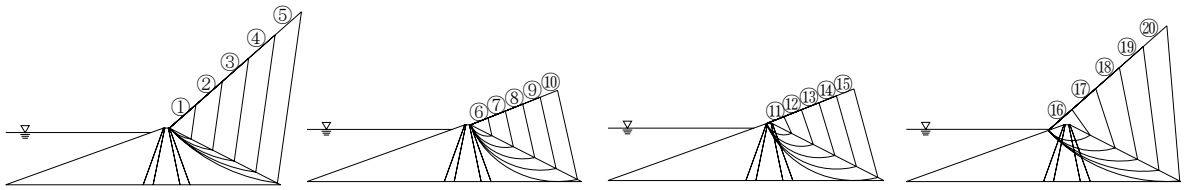

Figure 7. Downstream side slip circles of the limited number of slip circles

2.6.2 Method of setting the arbitrary slip circles

Figure 8 is a diagram of the grid partitions, which are the center points of the arbitrary slip circles. Figure 8 also shows an example of circles at one center point. As shown in Figure 8, the center points of the arbitrary slip circles were distributed including all center points of the limited number of slip circles. Next, for one grid point of one center point of circles, a minimum thick circle with radius 5m from the dam body surface was prepared as shown on the right side of Figure 8. Next, the radius of a circle was increased in increment of 5m. The circles were set in a range that does not exceed the maximum depth of the dam bottom. Approximately 2,600 and 2,200 circles were prepared in the upstream and downstream sides, respectively. In this paper, these circle groups are called the arbitrary slip circles.

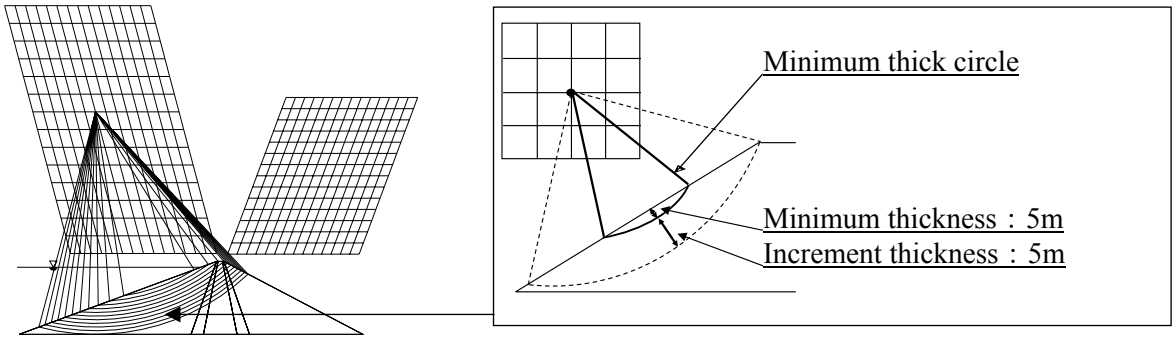

Figure 8. Explanatory diagram of the arbitrary slip circles

2.7 Sliding deformation analysis

Sliding deformation analysis was done using the strength material properties in Table 1 using the Newmark's method. The strength physical properties were set based on the c-φ method and the cohesion, c, was set as zero.

2.8 Analysis results

Figure 9 is a diagram showing the maximum response acceleration distribution in the upstream-downstream direction based on the seismic response analysis. Overall, the maximum response acceleration tends to decrease from the dam body bottom towards its surface. This is presumed to be a result of the non-linearity of the dynamic deformation properties of the dam body materials.

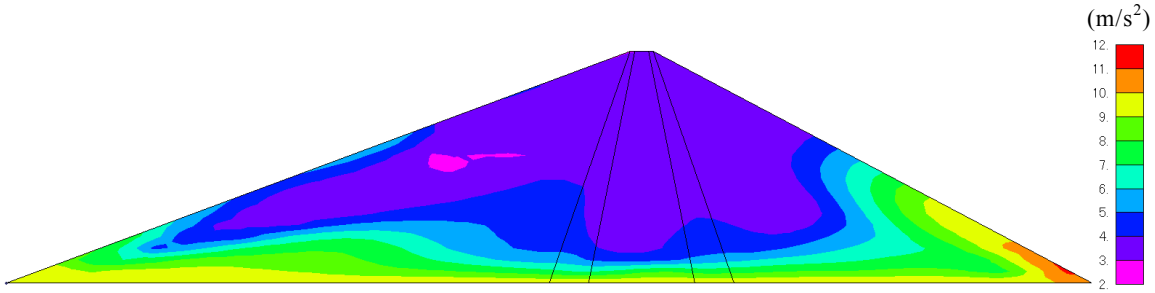

Figure 9. Maximum acceleration distribution in the upstream-downstream direction

The sliding deformation analysis results obtained by the Newmark's method are shown in Table 5 and circles on which the maximum sliding deformations are produced on the limited number of slip circles and the arbitrary slip circles are shown in Figure 10. The contour figure of Figure 10(b) shows the maximum sliding deformations by the arbitrary slip circles at all grid points.

In the limited number of slip circles on the upstream side, the maximum sliding deformation is produced on the shallow circle [1] that passes through only the rock zone, and the sliding deformation is 0.19m. In the arbitrary slip circles on the upstream side, the maximum sliding deformation is produced at the circle number 1590 in the high elevation on the slope surface, and the sliding deformation is 0.33m, which is 1.7 times larger than that of the circle [1] of the limited number of slip circles. It is assumed that the maximum sliding deformation based on the arbitrary slip circles is larger than that of the limited number of slip circles because among the limited number of slip circles on the upstream side, shallow small circles are not set on the high elevation of the saturated part with

smaller strength properties.
Among the limited number of slip circles on the downstream side, the maximum sliding deformation is produced on the shallow circle [5] that passes through only the rock zone, and the sliding deformation is 0.03m. Among the arbitrary slip circles on the downstream side, the maximum sliding deformation is produced at the circle number 2142 in the middle elevation of the slope surface, and the sliding deformation is 0.37, which is 12 times larger than that of the circle [5] of the limited number of slip circles. Similarly to the upstream side, the circle at which the maximum sliding deformation of the arbitrary slip circles on the downstream side is a shallow small circle on the middle elevation of the slope surface, which is not considered by the limited number of slip circles.

Table 5. The maximum sliding deformation by the limited number of slip circles and the arbitrary slip circles

Method of setting slip circles	Upstream side		Downstream side	
	Circle number	Maximum sliding deformation(m)	Circle number	Maximum sliding deformation(m)
limited number of slip circles	①	0.19	⑤	0.03
arbitrary slip circles	1590	0.33	2142	0.37

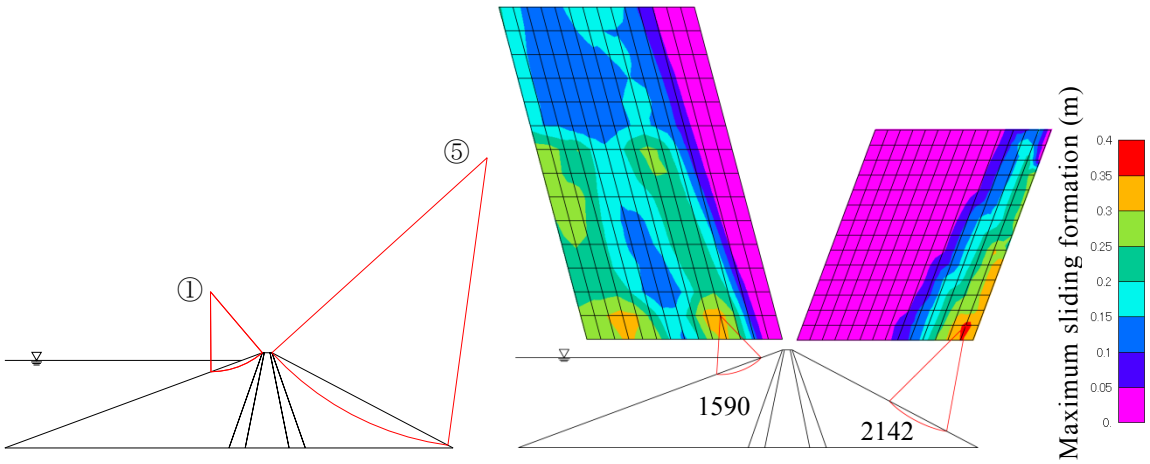

(a) limited number of slip circles (b) arbitrary slip circles

Figure 10. Circles of the maximum sliding deformation

2.9 Considerations of the effects of the arbitrary slip circles and the limited number of slip circles on the sliding deformations by the Newmark's method

The circles where the maximum sliding deformations occurred on the arbitrary slip circles are shallow circles on the slope surfaces both upstream and downstream. Here, the effects of the arbitrary slip circles on the maximum sliding deformation are considered.

Figures 11 and 12 show the results of the sliding deformations of the arbitrary slip circles with the horizontal axis of the circle number and the vertical axis of the sliding deformation of the circle categorized by the depth of the circles. The red lines shown in Figures 11 and 12 represent the maximum sliding deformation by the limited number of slip circles. Figures 11 and 12 show that the circles where the sliding deformations are larger than the red lines are often the minimum thick circles with depth from the dam body surface of 5m. This is assumed to be partly a result of using the strength physical properties at which cohesion is zero according to the c-φ method.

Figure 13(a) shows circles for which the sliding deformations by the arbitrary slip circles on the upstream side are 0.19m or larger. Figures 10(b) and 13(a) show that there are many shallow circles on the middle and high elevation of the slope surface, and there are also circles on the high elevation at the almost same location of the circle [1] where the maximum sliding deformation is produced by the limited number of slip circles. As shown in Figure 13(a), it is confirmed that even among circles in the middle and high elevation, the sliding deformation produced by the arbitrary slip circles is larger than that by the limited number of slip circles. On the downstream side, there are many circles where the maximum slip deformations exceed 0.03m as shown in Figure 13(b). Figure 13(c), which shows the circles at which the sliding deformations on the downstream side are 0.2m or larger, reveals that the circles are all concentrated at the middle elevation on the slope surface, and the maximum sliding deformations of the circles on the high elevation of the slope surface on the downstream side are between 0.03 and 0.2m.

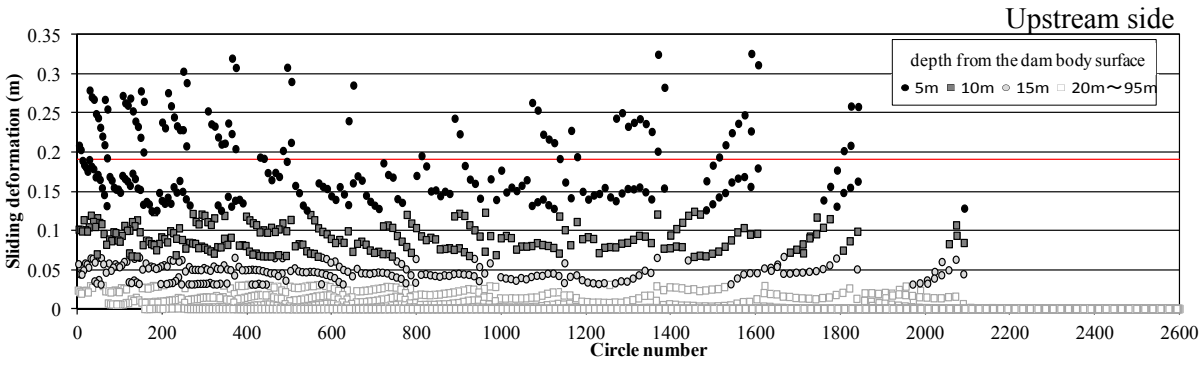

Figure 11. Sliding deformations of all circles prepared as arbitrary slip circles

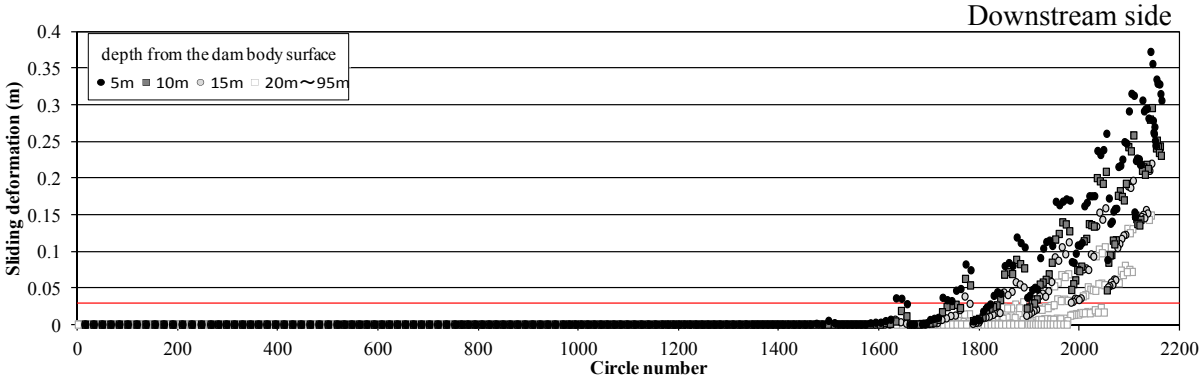

Figure 12. Sliding deformations of all circles prepared as arbitrary slip circles

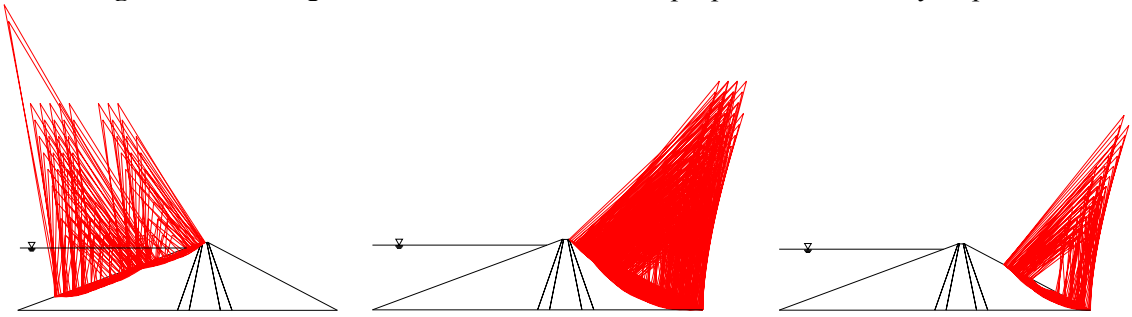

(a) Larger than 0.19m (b) Larger than 0.03m (c) Larger than 0.2m

Figure 13. Circles larger than a certain deformation (arbitrary slip circles)

3. CONCLUSIONS

The effects on the sliding deformation of the limited number of slip circles and the arbitrary slip circles were studied concerning the sliding deformation during a large earthquake at an earth core rockfill model dam by the Newmark's method. With both the limited number of slip circles and the arbitrary slip circles, the maximum sliding deformations were produced by shallow circles on the slope surfaces. The differences between the sliding deformations based on the limited number of slip circles and the arbitrary slip circles were about 1.7 times on the upstream side and about 12 times on the downstream side. It is assumed that one reason for the effects is the fact that shallow circles were not set in the saturated part at the middle and high elevation of the slope surfaces in the limited number of slip circles. Among circles which pass through the high elevation of the slope surfaces, sliding deformations calculated based on the arbitrary slip circles were larger than the maximum sliding deformations calculated based on limited number of slip circles.

In the future, analysis varying conditions such as slope gradient, maximum acceleration, input wave forms and material properties will be performed to further study on the effects of the limited number of slip circles and the arbitrary slip circles on the maximum sliding deformation.

REFERENCES

River Bureau, Ministry of Land, Infrastructure, Transport and Tourism (MLIT), (2005): *Guidelines for Seismic Performance Evaluation of Dams during Large Earthquakes (Draft),* Japan. (in Japanese)

Y. Yamaguchi, N. Tomida, and M. Mizuhara, (2009): *Influence Analysis and Simplified Estimation Method of Sliding Deformation of Rockfill Dams due to Large Earthquakes*, Research Report of Public Works Research Institute, No.212, pp.1-31, Public Works Research Institute, Japan. (in Japanese)

Y. Yamaguchi, N. Tomida and M. Mizuhara, (2005): *Effects of Sliding Circle on the Maximum Sliding Deformation of Rockfill Dams due to Large Earthquakes*, Engineering for Dams, No.229, pp.13-23, Japan Dam Engineering Center, Japan. (in Japanese)

Duncan, J. M. and Chang, C. Y., (1970): *Nonlinear analysis of stress and strain in soils*, Journal of the Soil Mechanics and Foundations Division, 96(SM5), pp.1629-1653, ASCE, USA.

Newmark, N.M., (1965): *Effects of earthquakes on dams and embankment*, Geotechnique, Vol.15, No.2, pp.139-173, USA.

Y. Sawada, T. Takahashi, A. Sakurai, and H. Yajima, (1977): *The Distribution Characteristics of The Material Properties and The Dynamic Behaviors of Rockfill Dams,* CRIEPI Research Report, 377008, pp.67-68, Central Research Institute of Electric Power Industry, Japan. (in Japanese)